CHARACTERISATION OF SELECTED GaAs THIN FILM PHOTOVOLTAIC STRUCTURES FOR CONCENTRATORS[*]

M. Ružinský[1], V. Šály

Slovak University of Technology, Faculty of Electrical Engineering and Information Technology, Ilkovičova 3, SK-81219 Bratislava, Slovak Republic

E. Aperathitis, Z. Hatzopoulos

Microelectronics Research Group, Institute of Electronic Structure & Laser, Foundation for Research and Technology – Hellas, P.O. Box 1527, Heraklion 71110, Crete, Greece

The molecular beam epitaxy is considered to be suitable method for preparation of efficient GaAs solar cells. This paper deals with GaAs p/i/n solar cell structures prepared with different thickness of intrinsic i-region. The current–voltage characteristics in the dark and the performance under standard simulated light spectra and concentrated light were investigated. The dielectric properties at the frequency range from 50 Hz to 1 MHz and at different temperatures were investigated, as well. Preliminary results on fully processed $1\,\text{cm} \times 1\,\text{cm}$ p/i/n GaAs solar cells have shown an increase in maximum power output by a factor of around 2.7 to 3.0 under concentrated illumination of 5 Suns. This work is being carried out as a part of an effort to fabricate efficient multiple quantum well GaAs cells based on thin film structures.

1   Introduction

Gallium–arsenide cells have been in race with silicon single-crystal for the highest efficiency photovoltaic (PV) device. GaAs has many desirable properties: it has an ideal direct band gap (1.43 eV), is highly absorptive and relatively insensitive to heat, it can be alloyed with many materials (aluminium, phosphorus, antimony, indium) and it is radiation resistant. The radiation resistance makes GaAs suitable for outer–space and concentrator applications. GaAs cells are not Auger limited and therefore their potential under concentrated light was as early as 1986 expected to reach efficiency 34 % [1]. GaAs has giving cells with a predicted efficiency up to 30 % at one sun – air-mass 1 (AM1) illumination, which, however, until now has not been realized [2, 3, 4]. Such efficiency for III–V based single-junction solar cells is constrained by the second law of thermodynamics [1, 5, 6].

---

[*]Presented at the Workshop on Solid State Surfaces and Interfaces II, Bratislava, Slovakia, June 20 – 22, 2000.
[1]E-mail address: ruzinskm@elf.stuba.sk

2   GaAs structures for solar cells

The GaAs layers are most frequently grown by using two popular techniques: molecular beam epitaxy (MBE) or metal-organic chemical vapour deposition (MOCVD). In MBE, a heated substrate wafer is exposed to gas-phase atoms of gallium and arsenic that condense on the wafer on contact and grow the thin GaAs film. In MOCVD, a heated substrate is exposed to gas-phase organic molecules containing gallium and arsenic, which react under the high temperatures, freeing gallium and arsenic atoms to adhere to the substrate. In both of these techniques single crystal GaAs layers grow epitaxially. This controlled growth results in a high degree of crystallinity and consequently in high cell efficiency.

One of the greatest advantages of GaAs and its alloys as PV cell materials is the wide range of design options possible. A cell with a GaAs base can contain several layers of slightly different compositions that allow a cell designer to control the generation and collection of charge carriers. One of the most common GaAs cell structures uses a very thin so–called window layer of AlGaAs on the top. In GaAs solar cells, the deteriorating effect of front surface recombination at short wavelengths can be seen, for example, by comparing quantum efficiencies of cells with and without a window layer [7].

The largest barrier to the success of GaAs cells has been high cost of a single-crystal GaAs substrate. Three approaches towards lowering the cost of GaAs devices have been explored [2]:

a) to fabricate cells on cheaper substrates like Si or Ge,

b) to grow cells on a removable GaAs substrate (that can be reused to produce other cells) and

c) to increase further the efficiency of the cell.

Single-junction GaAs cells restrict efficiency because their PV response is limited to a small part of the solar spectrum. Multijunction devices stack two or more cells on top of each other to capture more of solar light spectrum and they are capable of reaching efficiencies of 35 % also for thin film PV cells. Most high-efficiency multijunction devices are based on GaAs or its alloys and are made primarily for use under concentrated sunlight.

The p/i/n GaAs solar cell structure leaded to the idea to incorporate quantum wells (QW or in the multiple case MQWs) in the i-region in order to enhance its performance exploiting the photons with the energy lower than the band-gap of the semiconductor material. Such photons can be absorbed in the quantum wells. So far, an efficiency of 14 % has been reached on MQW GaAlAs structures [8].

3   Experimental conditions

In our work, we have investigated the behaviour of p/i/n GaAs solar cells in the dark as well as under standard and concentrated simulated sunlight in order to get information about the optimum structure which can be efficiently used in solar cells for terrestrial applications under concentrated sunlight. The solar cell structures, p/i/n GaAs, were grown by MBE on monocrystalline n^+ GaAs substrates. For investigating the influence of the i-region on the p/i/n GaAs solar cells output performance, three different types of cells were prepared. Details of the structure

can be seen in Table 1. The buffer and superlattice layers grown on the crystalline substrate serve to improve the back surface field (BSF) properties as well as for smoothing the interface between the GaAs substrate and the epitaxial layers of the structure grown on it. The window layer was a 30 nm thick $Al_{0.8}Ga_{0.2}As$, layer doped by Be. The antireflecting coating was SiN_x made by Plasma Enhanced Chemical Vapour Deposition (PECVD). The prepared types of cells had different thickness of the intrinsic d_i layer (Table 2).

Thickness	Material	Dopping
$0.6\,\mu m$	GaAs : Be – cap	$P = 1 \times 10^{25}\,m^{-3}$
30 nm	$Al_{0.8}Ga_{0.2}As$: Be – window	$P = 3 \times 10^{24}\,m^{-3}$
$0.3\,\mu m$	GaAs : Be emitter	
	GaAs (intrinsic)	
$2.6\,\mu m$	GaAs : Si – base	$N = 1 \times 10^{23}\,m^{-3}$
$20\times(2.8\,nm\,Al_{0.36}Ga_{0.64}As$: Si/2.7 nm GaAs : Si) – BSF		$N = 2 \times 10^{24}\,m^{-3}$
$1\,\mu m$	GaAs : Si – buffer	$N = 2 \times 10^{24}\,m^{-3}$
	GaAs : Si – substrate	$N = 2 \times 10^{24}\,m^{-3}$

Table 1. Details of the GaAs p/i/n solar cells structures

Sample	$d_i\,[\,\mu m]$	$d_b\,[\,\mu m]$	$d_i + d_b\,[\,\mu m]$
GS10	0	2.6	2.6
GS12	0.5	2.6	3.1
GS13	0.8	2.6	3.4

Table 2. The thickness of the base d_b and intrinsic layer d_i of the three prepared cells

(Ge/Au)/Ni/Au was used for n-ohmic contacts metallization which covered the back side of the n^+ GaAs substrate and (Pt/Ti)/Pt/Au for p-ohmic contacts, after activating the ohmic behaviour of the contacts in a rapid annealing system at 410 °C for 1 minute. All the processing of the devices was performed using standard photolithographic techniques. Both, dark and illumination measurements were made at room temperature. The solar simulator ORIEL model 6722 and radiometer ORIEL were used to illuminate the samples and to measure the irradiation, respectively. The solar cells were measured under the mentioned simulator light with xenon lamp at AM1.5 spectrum, 100 mW/cm^2 and at concentrated light 500 mW/cm^2 conditions. The dark characteristics of the devices current–voltage (I–V) and capacitance–voltage (C–V) curves as well as the performance of the devices under standard and concentrated sunlight were examined on samples – solar cells of 1 cm $\times$ 1 cm area having 14 lines/cm as top contact grid. Capacitance measurements were performed in frequency range from 50 Hz to 1 MHz at different temperatures using HIOKI Z Tester.
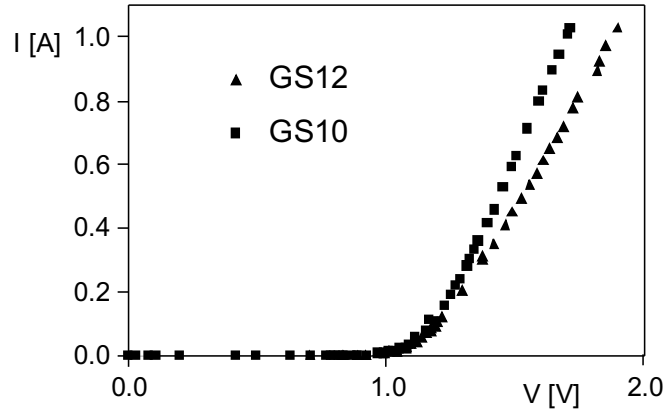
Fig. 1. Current–voltage characteristics of the chosen samples in the dark
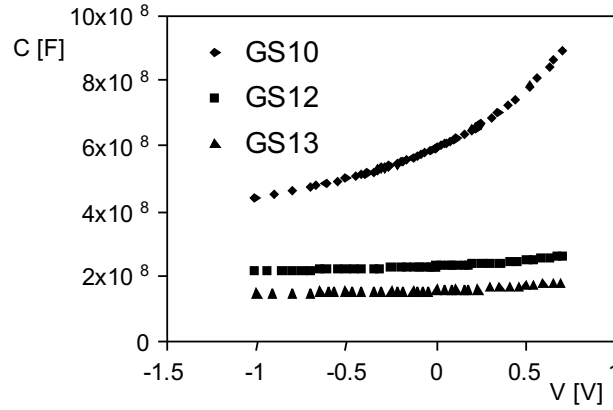
Fig. 2. C–V curves of the three samples measured at 1 kHz

4   Results and discussion

4.1   Characteristics in the dark

Fig. 1 shows the measured dark current–voltage characteristics at room temperature of the p/i/n samples with two different i-region thicknesses. Generally, the dark current–voltage curve of the p-n junction in a forward direction can be expressed by the exponential voltage dependence

$$I = I_{sat} \exp\left(\frac{qV}{nkT}\right) \tag{1}$$

where I_{sat} is a saturation current, q is the charge of an electron, n is the ideality factor, k is the Boltzmann constant and T [K] is the temperature. The measured characteristics deviate more
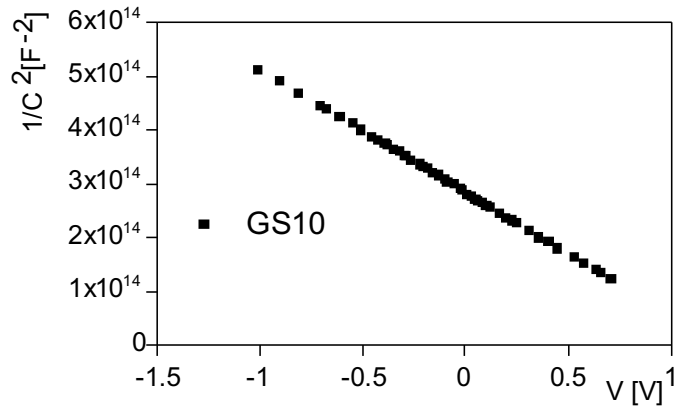
Fig. 3. The dependence of $1/C^2$ *vs* voltage of the sample without i region
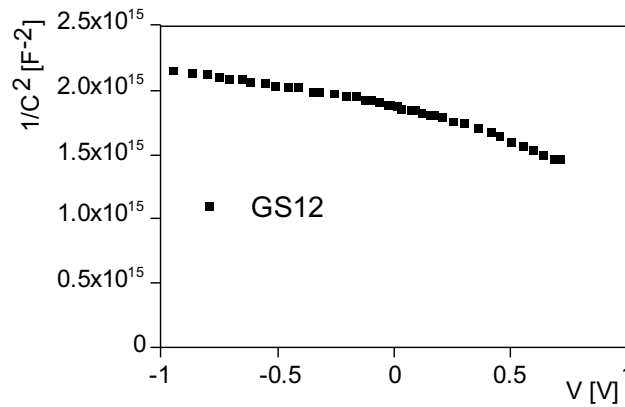
Fig. 4. Non-linear dependence of $1/C^2$ *vs* voltage of the p/($i = 0.5\mu$m)/n sample

or less in comparison to the equation (1). The ideality factor is a voltage dependent parameter, varies from $n = 1$ to $n = 2$ and revealing the recombination processes at the interface. The value $n = 2$ dominates at low currents, while at higher currents the value $n = 1$ dominates. The other p-n junction parameters, mainly series resistance and shunt conductance, affect the shape of the I–V curve, as well. The abruptness of the I–V curves and consequently the value of n depends on the i-region thickness but no functional dependence can be identified for the three different i-region thicknesses investigated in this work.

In order to evaluate the barrier height, the capacitance of biased samples were measured at the *ac* signal of 50 mV and the C–V curves are shown in Fig. 2. The dependencies of $1/C^2$ *vs* voltage, usually straight lines in reverse direction, are depicted in Fig. 3 and Fig. 4. A space charge region of thickness x_b in p-n or p/i/n structure behaves as a dielectric with dielectric permittivity ϵ_r and an area of A (area of the junction). The barrier thickness x_b is a function of
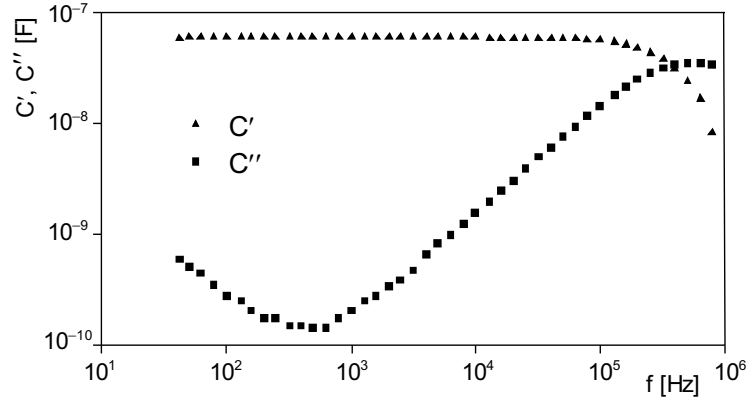
Fig. 5. An example of the real C' and imaginary C'' parts of complex capacitance at room temperature

bias voltage V. Under reverse bias, the depletion-region capacitance dominates the total diode capacitance C [9],

$$C = \frac{dQ}{dV} = A \left(\frac{q\epsilon_r\epsilon_0 N_D}{2(V_D + V)} \right)^{\frac{1}{2}} \tag{2}$$

where V_D is the diffusion voltage ϵ_0 and ϵ_r is permittivity of vacuum and material, respectively and N_D is the concentration. The value of V_D can be deduced in the case of abrupt junction from the intersection of the extrapolated $1/C^2$ *vs* V curve (if it is linear) with the horizontal axis (Fig. 3). The value of $V_D = 1.23\,\text{V}$ was deduced from Fig. 3 for the p/n GaAs sample ($i = 0\,\mu\text{m}$). The $1/C^2$ *vs* voltage curve deviates from the straight line form when the diffusion voltage is dependent on the bias or in the case of a p-n junction which is not abrupt. Such behaviour can be seen in Fig. 4, where the $1/C^2$ *vs* voltage has been plotted for the p/i/n sample with $i = 0.5\,\mu\text{m}$.

The trapping and de-trapping processes at deep levels in a semiconductor space charge region at p-n junction or Schottky barrier represent an exact analogy of dipolar polarization in dielectrics, since the delayed emission of electrons from traps and their subsequent rapid transport to the quasi-neutral bulk material represent an identical process to the reorientation of a molecular dipole, with the characteristic relaxation time. A finite value capacitance ΔC adds to space charge region capacitance, since the number of traps is finite. A frequency dependence of the parts of complex capacitance at room temperature is shown in Fig. 5. The real part of capacitance C' is frequency independent in a quite wide range of frequencies. An indication of loss peak could appear at the high frequencies of imaginary part of the complex capacitance C'' but the frequency range was limited by the bridge used for this measurement. A frequency independent C' and increasing C'' toward low frequencies indicate a *dc* process rather than low frequency dispersion often observable in many dielectric systems at low frequencies [10] when
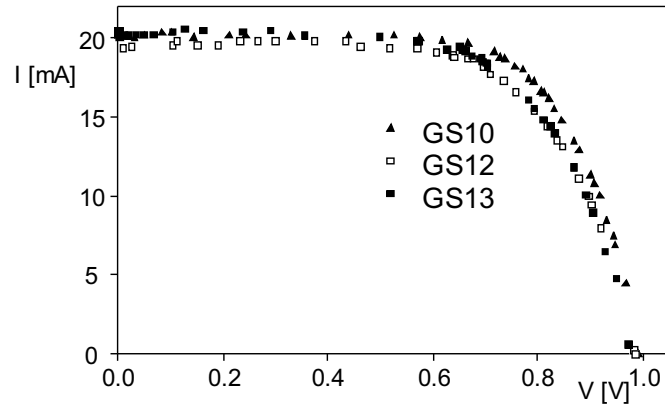
Fig. 6. Current–voltage characteristics of chosen samples at standard illumination
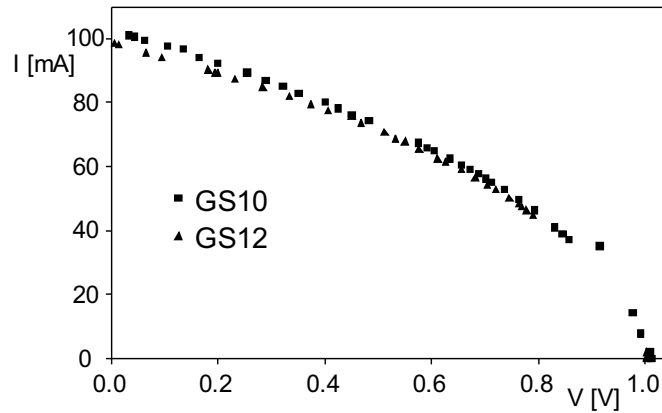
Fig. 7. Current–voltage characteristics of chosen samples at 5 sun illumination

C' increases, as well, often with the same slope like C''. With increasing temperature the shape of curves does not change but they move slightly to higher frequencies.

4.2   Characteristics under illumination

The current–voltage characteristics of the samples under the simulated one-sun and five-suns AM1.5 illumination are shown in Figs. 6 and 7, respectively. Preliminary results of the p/i/n GaAs solar cells processed as 1 cm × 1 cm solar cell device have shown that an increase of performance (maximal output power P_{max}) by a factor of about 2.7 to 3.0 under concentrated simulated irradiation of 5 Suns is achievable. The short-circuit current I_{sc} was increased by a factor of 5 while the open-circuit voltage V_{oc} increased insignificantly. The increasing illumination level produced photo-generated electron-hole pairs while the temperature of the solar cell sam-

ple increases. The open-circuit voltage changes only slightly when the energy gap changes with changing temperature.

The decrease of fill factor FF ($FF = P_{max}/(V_{oc}I_{sc})$, P_{max} is the maximum power generated by the cell) at concentrated light resulte in decrease of efficiency from about 13 % at one sun to about 7.8 % at 5 suns. We suppose the higher series resistance R_s can be the reason of such performance damage. The higher voltage drop on R_s at higher current results in the decreasing of FF.

The investigation of p/i/n GaAs solar cells with different i region thickness in this work should serve as a primary work for preparation efficient MQW solar cell.

References

[1] D. E. Arvizu: in *Proc. 7th European Photovoltaic Solar Energy Conference*, Sevilla, Spain, 1986, p. 771

[2] L. L. Kazmerski: *Renewable and Sustainable Energy Reviews* **1** (1997) 71

[3] X. Tang *et al.*: in *Proc. 8th Photovoltaic Solar Energy Conference*, May 1988, Florence, Italy, 1988, p. 1497

[4] G. Cook *et al.*: *Photovoltaic Fundamentals*, U.S. DOE, Washington, 1991

[5] M. B. Prince: *J. Appl. Phys.* **26** (1955) 534

[6] J. J. Loferski: *J. Appl. Phys.* **27** (1956) 777

[7] Solar Cells: in *Wiley Encyclopedia of Electrical and Electronics Engineering* **19**, ed. J. G. Webster, John Wiley and Sons, Inc. New York, 1999, p. 618

[8] G. Haarpaintner *et al.*: in *Proc. 1st World Conference on Photovoltaic Energy Conversion*, December 1994, Waikoloa, Hawaii, 1994, p. 1783

[9] M. A. Green: *Solar Cells*, Prentice-Hall Inc., 1982

[10] S. H. Zaidi, A. K. Jonscher: *Semicond. Sci. Technol.* **2** (1987) 587